

NUMERICAL VERIFICATION OF TIME-DOMAIN MOMENT METHOD IN ULTRASOUND TOMOGRAPHY

Yue Wang[†] and Joel M. Morris[‡]

[†]Georgetown University, Division of Imaging Science and Information Systems, Washington, DC 20007; [‡]University of Maryland Baltimore County, Department of Computer Science and Electrical Engineering, Baltimore, Maryland 21228

(Paper JBO-047 received Oct. 12, 1995; revised manuscript received Feb. 27, 1996; accepted for publication Mar. 3, 1996.)

ABSTRACT

In ultrasound tomography the time-domain moment method is very promising in that it has been shown to yield a close agreement between the time-spatial moment expansion and the true field representation. This paper introduces a numerical technique to compute the analytical solution for forward scattering by using a Bessel function series and the inverse discrete Fourier transform, and shows that the artifacts that occur are due to convolution aliasing and undersampling aliasing. Computer simulation has reconstructed these two types of aliasing separately, and has shown that they can be removed by a properly designed algorithm. This alias-free numerical solution is used to verify Cavicchi's moment-method formulation. A significant improvement in numerical verification is then obtained. © 1996 Society of Photo-Optical Instrumentation Engineers.

Keywords medical imaging; ultrasound tomography; scattering; moment method; signal processing; aliasing artifact.

1 INTRODUCTION

Ultrasonic diffraction tomography, still in its research stages, is a computed imaging technique for identifying the interaction between an incident field and scattered objects. In medical imaging applications, the ultrasound inverse scattering procedure has been studied intensively in the frequency domain in the past two decades.¹⁻² However, phase wrapping has been proven to be a fundamental problem in these approaches: when the phase differences between waves propagating through a relatively homogeneous medium and those propagating through the strong scatterer exceed $\pm\pi$, the information required to reconstruct the scatterer is lost. Consequently, the time-domain moment method introduced recently by Cavicchi appears to be very promising because it is a nonlinear higher-order inverse scattering procedure that inherently retains all information in the field representation.³

Some preliminary numerical studies based on Cavicchi's discrete time-spatial expansion of the acoustic inhomogeneous wave equation have shown good agreement between the temporal-moment method approximation and the "true" solution for forward scattering, in which the agreement between these two solutions was measured by the average inner product (perfect alignment yields a value of 1). By closely investigating the data, we found that the lack of perfect agreement in

the computer simulations, with average inner product values of 0.8 to 0.9, was mainly due to distortions in the numerical "true" field representation.⁴

The primary purpose of this paper is to show that two sources of aliasing contribute to this distortion. One source is due to the use of circular convolution when in fact linear convolution is required, and the other is due to undersampling in the frequency domain when the Bessel function series discretization is used. The underlying mathematics will be reviewed in Sec. 2. In Sec. 3, a computer simulation procedure is presented to reconstruct these two different aliasing effects separately to verify that the ripples observed ahead of the wavefront are due to aliasing, and to show that the artifacts can be removed by a well-designed algorithm. Also in Sec. 3, the beneficial effects of these corrections will be demonstrated by showing that the alias-free numerical representation of the "true" field leads to a better agreement with the moment method approximation. Some conclusions will be presented in Sec. 4.

2 MATHEMATICAL BACKGROUND

Consider two-dimensional forward scattering. Let the total field strength and the scattered field strength at position (x,y) and time t be represented by the scalar functions $p^{\text{tot}}(x,y,t)$ and $p^{\text{sc}}(x,y,t)$, respectively. According to scalar diffraction theory,

Address all correspondence to Yue Wang.
E-mail: yuewang@isis.imac.georgetown.edu

the wave propagation must satisfy the time-dependent linear inhomogeneous lossless scalar wave equation

$$\begin{aligned} & \left(\frac{\partial^2}{\partial x^2} + \frac{\partial^2}{\partial y^2} - \frac{1}{c_0^2} \frac{\partial^2}{\partial t^2} \right) p^{\text{sc}}(x, y, t) \\ & = - \left(\frac{1}{c_0^2} - \frac{1}{c^2(x, y)} \right) \frac{\partial^2}{\partial t^2} p^{\text{tot}}(x, y, t) \quad (1) \end{aligned}$$

at each source-free point, where c_0 is the free-space speed of sound, and $c(x, y)$ is the spatially varying speed of sound. The relation [Eq. (1)] is known as the *Helmholtz equation*. By applying Green's function, the theoretical solution to the above equation is given by the Lippmann-Schwinger equation:^{3,5}

$$\begin{aligned} p^{\text{sc}}(x, y, t) &= \int_{-\infty}^{\infty} \int_{-\infty}^{\infty} \int_{-\infty}^{\infty} \left[\frac{1}{c_0^2} - \frac{1}{c^2(x', y')} \right] \\ & \quad \times \frac{\partial^2}{\partial t'^2} [p^{\text{tot}}(x', y', t')] \\ & \quad \times G(x, y, t | x', y', t') dx' dy' dt', \quad (2) \end{aligned}$$

where $G(\cdot)$ is Green's solution given by

$$\begin{aligned} & G(x, y, t | x', y', t') \\ &= \frac{H\{t - t' - 1/c_0[(x - x')^2 + (y - y')^2]^{1/2}\}}{2\pi\{(t - t')^2 - [(x - x')/c_0]^2 - [(y - y')/c_0]^2\}^{1/2}} \quad (3) \end{aligned}$$

and $H(\cdot)$ is the Heaviside step function. Under the time-spatial moment method expansion, Eq. (2) can be rewritten as^{4,6}

$$\begin{aligned} & p^{\text{inc}}(n_t, n_x, n_y) \\ &= p^{\text{tot}}(n_t, n_x, n_y) - \frac{c_0}{2\pi\Delta t} \\ & \quad \times \sum_{n_{t'}=1}^{n_t-1} \sum_{n_{x'}=1}^{N_{xy}} \sum_{n_{y'}=1}^{N_{xy}} I_{\phi}(n_{tt'}, n_{xx'}, n_{yy'}) \\ & \quad \times \left[\frac{1}{c_0^2} - \frac{1}{c^2(n_{x'}, n_{y'})} \right] \\ & \quad \times \sum_{m=-N_f}^{N_f} h_f(m) p^{\text{tot}}(n_{t'} - m, n_{x'}, n_{y'}), \quad (4) \end{aligned}$$

with

$$\begin{aligned} n_{xx'} &= n_{x'} - n_x + N_{xy}, \\ n_{yy'} &= n_{y'} - n_y + N_{xy}, \\ n_{tt'} &= n_t - n_{t'}, \quad (5) \end{aligned}$$

and p^{inc} is the incident field, Δt is the temporal sampling interval, N_{xy} denotes the total number of

pixels along either the x or y axis, N_f denotes the size of filter window, I_{ϕ} is the integration of the basis function ϕ against the Heaviside step function, and $h_f(m)$ is a second-order digital differential filter. Let p^{inc} be expressed by

$$\begin{aligned} & p^{\text{inc}}(n_t, n_x, n_y) \\ &= \sum_{n_{t'}=1}^{n_t-1} \sum_{n_{x'}=1}^{N_{xy}} \sum_{n_{y'}=1}^{N_{xy}} A_{i,j} p^{\text{tot}}(n_{t'}, n_{x'}, n_{y'}), \quad (6) \end{aligned}$$

where the matrix elements $A_{i,j}$ are required to satisfy the matrix equation

$$\mathbf{p}^{\text{inc}} = \mathbf{A} \cdot \mathbf{p}^{\text{tot}}. \quad (7)$$

Then, mathematically, the transient response p^{tot} can be obtained from information of I_{ϕ} , $c(x, y)$ and p^{inc} . Based on the same field expansions, an iterative inverse scattering procedure for reconstructing the scatterer is very desirable.

In the test case of the scattering inside and outside an infinite-length circular cylinder, an independent analytical "true" solution is numerically synthesized by first calculating the impulse response of the scattered field from the well-known Bessel function series solution, and then applying the inverse discrete Fourier transform (IDFT) in the light of the actual incident field. Let the incident field be a Gaussian-damped sinusoidal plane wave given by

$$\begin{aligned} & p^{\text{inc}}(x, y, t) = \exp[-(c_0^2/\sigma^2)(t - x/c_0)^2] \\ & \quad \times \sin[\Omega_0(t - x/c_0)]u(t - x/c_0) \quad (8) \end{aligned}$$

with its DFT representation

$$p_d^{\text{inc}}(k) = \sum_{n=0}^{N_t-1} p^{\text{inc}}(n\Delta t) \exp(-j2\pi nk/N_t), \quad (9)$$

and let the sampled Fourier representation of the Bessel function series solution be given by^{4,7}

$$\begin{aligned} & p_i^{\text{sc}}(x, y, \Omega) \Big|_{\Omega=2\pi k/N_t\Delta t, r^2=x^2+y^2} \\ &= \begin{cases} \sum_{m=0}^{\infty} S_m H_m^{(2)}(\Omega/c_0\sqrt{x^2+y^2}) \\ \quad \times \cos[mtg^{-1}(y/x)], & r \geq a, \\ \sum_{m=0}^{\infty} W_m J_m(\Omega/c_1\sqrt{x^2+y^2}) \\ \quad \times \cos[mtg^{-1}(y/x)], & r < a \end{cases}, \quad (10) \end{aligned}$$

where

$$\begin{aligned} & S_m = -\frac{2}{\Delta_m} [J_m(a\Omega/c_1) \\ & \quad \times [J_{m+1}(a\Omega/c_0) - J_{m-1}(a\Omega/c_0)] - J_m(a\Omega/c_0) \\ & \quad \times [J_{m+1}(a\Omega/c_1) - J_{m-1}(a\Omega/c_1)]] \quad (11) \end{aligned}$$

$$W_m = \frac{2}{\Delta_m} [J_m(a\Omega/c_0)[H_{m+1}^{(2)}(a\Omega/c_0) - H_{m-1}^{(2)}(a\Omega/c_0)] - H_m^{(2)}(a\Omega/c_0) \times [J_{m+1}(a\Omega/c_0) - J_{m-1}(a\Omega/c_0)], \quad (12)$$

and

$$\Delta_m = J_m(a\Omega/c_1)[H_{m+1}^{(2)}(a\Omega/c_0) - H_{m-1}^{(2)}(a\Omega/c_0)] - H_m^{(2)}(a\Omega/c_0)[J_{m+1}(a\Omega/c_1) - J_{m-1}(a\Omega/c_1)]. \quad (13)$$

Then, from the Fourier convolution theorem, the temporal scattered field can be calculated through the IDFT operation given by:

$$p^{sc}(x, y, n) = \frac{1}{N_t \Delta t} \sum_{k=0}^{N_t-1} p^{sc}(x, y, k) \exp(j2\pi nk/N_t), \quad (14)$$

where

$$p^{sc}(x, y, k) = \Delta t \cdot p_i^{sc}(x, y, k) \cdot p_d^{inc}(k). \quad (15)$$

Note that a result similar to Eq. (10) appears in Ref. 6, but it is for a cylindrical incident wave and is in terms of a polar coordinator system. Also, in Cavicchi's paper,³ Eq. (A15) is missing the factor $(\Delta t)^{-1}$ and Eq. (A10) has an erroneous expression. From signal processing theory, this discrete solution is of course subject to the aliasing effects of undersampling (determined by Δt or $\Delta\Omega$) and the smearing effects of windowing (determined by N_t).

3 SIMULATION AND ANALYSIS

Our simulation study and aliasing analysis of the test case included Cavicchi's moment method approximation, the numerical "true" field representation, and the alias-free numerical verification. The parameter setup was the same as Cavicchi's^{3,6}: $\Omega_0=1.0$ M Hz, $\sigma=2.0$ mm, $a=1.5$ mm, $c_1=0.5$ mm/ μ s, $c_0=1.0$ mm/ μ s, $f_s=19$ M Hz, $N_{xy}=64$, $N_t=256$, and $\Delta l=2.0$ $c_0\Delta t$. For simplicity, a three-point central differential approximation is currently used to implement the second-order digital differential filter $h_j(m)$, and I_ϕ is specified as

$$I_\phi(n_{tt'}, n_{xx'}, n_{yy'}) = \int_0^{2\pi} \int_0^{c_0\Delta t n_{tt'}} \phi[r \cos\theta - n_{xx'}\Delta l] \phi[r \sin\theta - n_{yy'}\Delta l] \times \frac{1}{[(c_0\Delta t n_{tt'})^2 - r^2]^{1/2}} \times r dr d\theta. \quad (16)$$

The total field values $p^{tot}=p^{inc}+p^{sc}$ from the moment method expansion were compared with the numerical "true" solution in terms of spatially nor-

malized inner products in order to evaluate the degree of agreement, where the spatially normalized inner product is defined by

$$\mathbf{p}^{tot}(n_t, n_x, n_y) \wedge \mathbf{p}^{tot}(n, x, y) = \frac{\sum_{n_x=1}^{N_{xy}} \sum_{n_y=1}^{N_{xy}} p^{tot}(n_t, n_x, n_y) \cdot p^{tot}(n, x, y)}{\sqrt{\|\mathbf{p}^{tot}(n_t, n_x, n_y)\| \cdot \|\mathbf{p}^{tot}(n, x, y)\|}}. \quad (17)$$

For our test experiment, the average inner product values are 0.876 and 0.924 at two different time snapshots. These values indicate less than perfect alignment. Figure 1 shows the "true" total field representation in which some ripples due to aliasing effects are noticeable ahead of the wavefront.

To identify the aliasing sources, we consider the complete computational procedure for obtaining the "true" scattered field. From digital signal processing theory, Eq. (14) can be rewritten as

$$p^{sc}(x, y, n) = \frac{1}{N_t \Delta t} \sum_{k=1}^{N_t-1} \left\{ \int_{-\infty}^{\infty} p^{sc}(x, y, \tau) \times \exp[-(j2\pi k\tau/N_t\Delta t)] d\tau \right\} \times \exp(j2\pi kn/N_t) = \int_{-\infty}^{\infty} p^{sc}(x, y, \tau) \frac{1}{N_t \Delta t} \times \sum_{k=1}^{N_t-1} \exp(j2\pi k(n - \tau/\Delta t)/N_t) d\tau$$

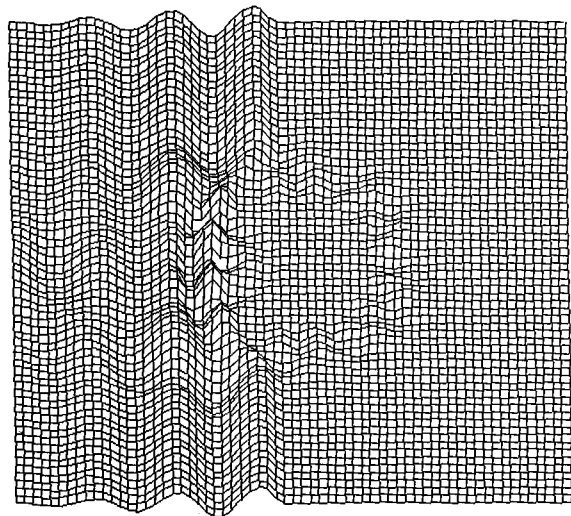


Fig. 1 Numerical "true" field representation at time snapshot $t_0+75\Delta t$. The incident field is a Gaussian-damped sinusoid spatial plane wave pulse propagating into the cross section of the cylinder object from the left to the right (along the x axis). The ripples noticeable ahead of the wavefront clearly indicate the effects of aliasing.

$$\begin{aligned}
 &= \int_0^{N_t \Delta t} \left[\sum_{m=-\infty}^{\infty} p^{sc}(x, y, \tau + m N_t \Delta t) \right] \\
 &\quad \times \frac{\sin[\pi(n \Delta t - \tau) / \Delta t]}{\sin[\pi(n \Delta t - \tau) / N_t \Delta t]} \\
 &\quad \times \exp[j\pi(n \Delta t - \tau)(N_t - 1) / N_t \Delta t] d\tau.
 \end{aligned} \tag{18}$$

Hence, this multiple reflection scattering clearly indicates that two sources of aliasing need to be taken into account, namely, undersampling aliasing and circular convolution aliasing. In Eq. (15) the frequency representation of the scattered field includes two components: the impulse response $p_i^{sc}(x, y, k)$, which is directly sampled from a continuous-frequency signal, and the incident field $p_d^{inc}(k)$, which is the DFT of a continuous-time signal. Undersampling aliasing in both the time and frequency domains may be introduced if the Heisenberg uncertainty constraint on the sampling resolution in the time and frequency domains is not satisfied.⁷ In addition, from direct application of the IDFT given by Eq. (14), circular convolution aliasing may occur in the scattered field $p^{sc}(x, y, n)$ because, in fact, linear convolution is required.

Figure 2 shows both circular-convolution aliasing and undersampling aliasing effects as a function of time at a fixed spatial position. We designed an algorithm to reconstruct and remove these two aliasing effects separately and thereby obtain a clean "true" field representation. The basic principle is

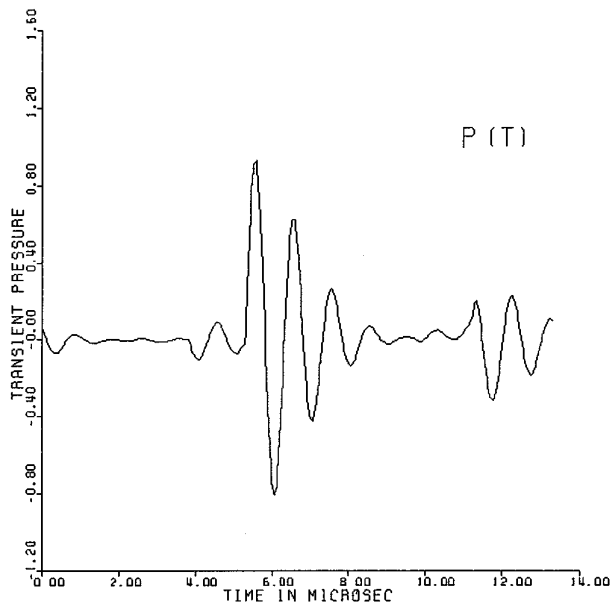


Fig. 2 Alias-response signal at a fixed spatial position as a function of time in a temporal window ($N_t=256$). The multiple reflections of the scattering field in this diffraction case are clearly observed. With a relation to the spatial domain, aliasing can be detected in the time domain.

that, for reconstructing undersampling aliasing, we use zero padding to eliminate the effect of circular-convolution aliasing so that the mislocations of the impulse response can be clearly detected; on the other hand, for reconstructing circular-convolution aliasing, we first open a window in the time domain sufficiently wide to include all significant reflection pulses, and then apply circular convolution to the window used previously.⁸ Figure 3 shows the undersampling aliasing effect where some reflection signals have been relocated ahead of the main scattering, and Figure 4 shows that circular convolution generates additional aliasing effects. Figure 5 shows the clean signal obtained by jointly imposing critical-sampling constraints (satisfying the Heisenberg uncertainty constraint when the maximum frequency value is given) and using a zero-padding technique.

By using our alias-free "true" field data, a new numerical verification for the Cavicchi's moment method expansion has shown a better agreement with higher inner-product values of 0.934 and 0.936 at the corresponding time snapshots, respectively. Figure 6 illustrates the alias-free scattered field that served as a reference for our verification.

4 CONCLUSION

In this paper, we designed and proposed an algorithm so that an alias-free numerical "true" field representation can be efficiently calculated to verify the time-domain moment method in ultrasound tomography. We presented a general form for numerical implementation of the scattered field in terms of a triple convolution computation [Eq. (18)],

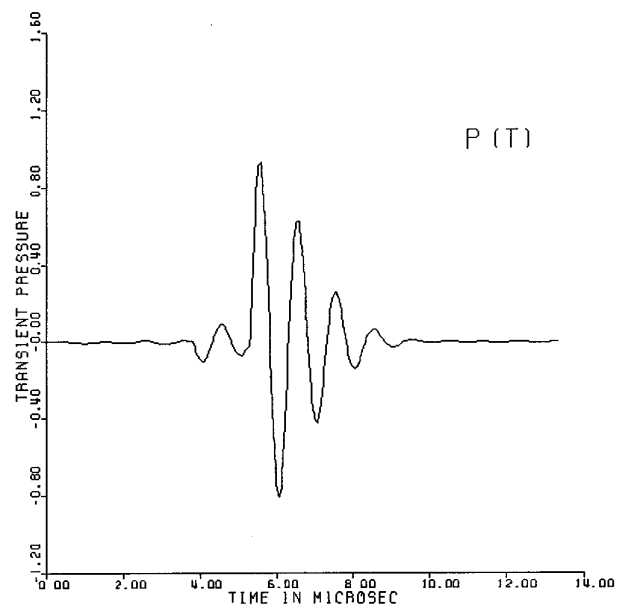


Fig. 3 Reconstructed-response signal with only undersampling aliasing.

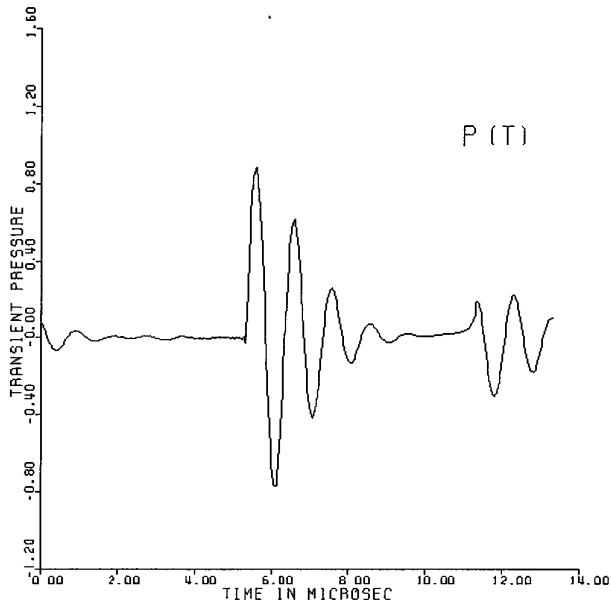


Fig. 4 Reconstructed-response signal with only convolution aliasing.

and a new formulation of the discrete Bessel function series solution for a plane wave response in a rectangular coordinate system [Eqs. (10) to (13)]. Using both theoretical analysis and computer simulations, we determined that the previous less than perfect agreement (with the average inner-product range of 0.8 to 0.9) in numerical verification was mainly due to the effects of undersampling aliasing and circular-convolution aliasing in the "true" scat-

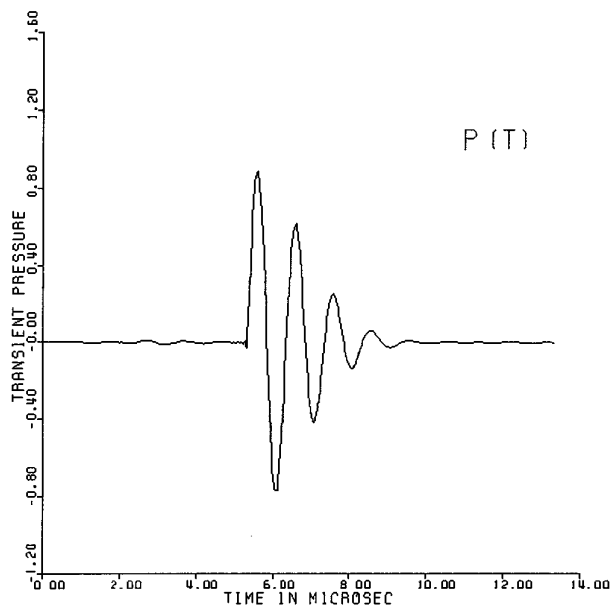


Fig. 5 Clean-response signal without aliasing generated by the well-designed new algorithm, where critical-sampling and zero-padding techniques are jointly imposed.

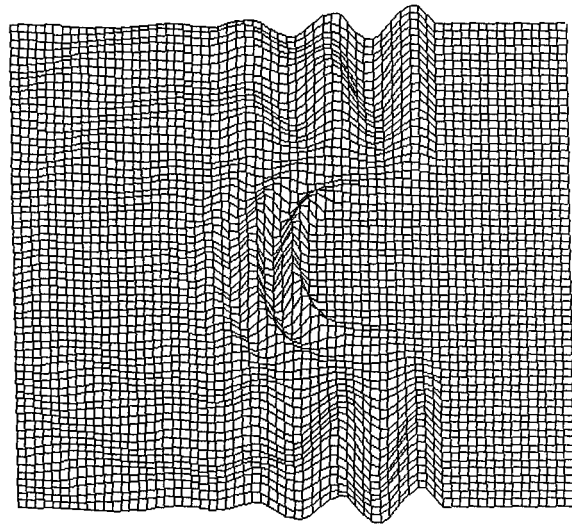


Fig. 6 Alias-free "true" total field representation at time snapshot $t_0 + 108\Delta t$, resulting from using the newly developed algorithm. The new result is considered as an alias-free estimate of the exact field solution, and is used as a reference in our numerical verification against the time-spatial moment expansion solution.

tered field representation. This result has led to a new artifact-free algorithm and has shown significant improvement in numerical verification by providing a higher average inner-product value of 0.94. Our analysis technique not only supports Cavicchi's time-domain moment method expansion approach, but is also of great practical importance for confidently evaluating the performances of other new algorithms, such as the quantum mechanics inverse method,⁹ without the Born approximation.

Acknowledgment

The authors would like to thank Thomas J. Cavicchi for stimulating the interest that led to this work. The authors are especially grateful to Dr. Michael L. Johnson, and the anonymous reviewer for their careful review and suggestions to improve the paper. Thanks are also due to Susan Kirby for her editorial assistance.

REFERENCES

1. J. F. Greenleaf, S. A. Johnson, S. L. Lee, G. T. Herman, and E. H. Wood, "Algebraic reconstruction of spatial distributions of acoustic absorption within tissue from their two-dimensional acoustic projections," *Acoustical Holography*, Vol. 5, pp. 591-603, Plenum Press, New York (1974).
2. J. F. Greenleaf, "Computerized tomography with ultrasound," *Proc. IEEE* **71**(3), 330-337 (1983).
3. T. J. Cavicchi, "Transient high-order ultrasonic scattering," *J. Acoust. Soc. Am.* **88**(2), 1132-1141 (August 1990).
4. Y. Wang and J. M. Morris, "Alias-free numerical verification of time domain approach in ultrasonic tomography," *Recent Developments in Biomedical Engineering*, J. Vossoughi, Ed., pp. 780-783, University of the District of Columbia, Washington, D.C. (1994).
5. S. Pourjavid and O. Tretiak, "Ultrasound imaging through time-domain diffraction tomography," *IEEE Trans. Ultrason. Ferroelec. Freq. Control* **38**(1), 74-84 (January 1991).
6. T. J. Cavicchi and W. D. O'Brien Jr., "Acoustic scattering of

- an incident cylindrical wave by an infinite circular cylinder," *IEEE Trans. Ultrason. Ferroelec. Freq. Control* **35**(1), 78–80 (January 1988).
7. S. Finette, "A computer model of acoustic wave scattering in soft tissue," *IEEE Trans. Biomed. Eng.* **34**(5), 336–344 (May 1987).
 8. C. R. Crawford, "CT filtration aliasing artifacts," *IEEE Trans. Med. Imaging* **10**(1), 99–102 (March 1991).
 9. K. J. Langenberg, D. Huo, and H. Morbitzer, "Towards quantitative ultrasonic imaging," in *Proc. IEEE Engineering in Medicine and Biology Society*, 11th Annual International Conference, pp. 400–401 (1989).